MCP Papers in Press. Published on June 29, 2015 as Manuscript M115.048413

Quantitative proteomics reveals the roles of peroxisome-associated proteins in anti-viral innate immune responses

Mao-Tian Zhou[1, §], Yue Qin[1,2, §], Mi Li[1,2], Chen Chen[1], Xi Chen[3],

Hong-Bing Shu[1, 2*], Lin Guo[1*]

[1]State Key Laboratory of Virology, College of Life Sciences

[2]Medical Research Institute

Wuhan University

[3]Wuhan Institute of Biotechnology, Wuhan, China

[§]M. Z and Y. Q. contributed equally to this work

*To whom correspondence should be addressed:

Dr. Hong-Bing Shu

Email: shuh@whu.edu.cn

Tel: +86-27-68753795

Dr. Lin Guo

E-mail: guol@whu.edu.cn

Tel: +86-27-68753800

Abbreviations

PEFs (peroxisome-enriched fractions); SeV (Sendai virus); MAC (membrane attack complex); MAM (mitochondrial-associated membranes); MHC (major histocompatibility complex); TLRs (Toll-like receptors); NLRs (NOD-like receptors); RLRs (RIG-I-like receptors); IFN (interferon); MOI (multiplicity of infection); FDRs (false discovery rates); SCX (strong cation exchange); ISRE (interferon-sensitive response element) ; NF-κB (nuclear factor kappa-light-chain-enhancer of activated B cells); GO (gene ontology); AP-2 (adaptor protein complex 2); IRF-1 (interferon regulatory factor 1)

Abstract

Compared to whole-cell proteomic analysis, subcellular proteomic analysis is advantageous not only for the increased coverage of low abundance proteins but also for generating organelle-specific data containing information regarding dynamic protein movement. In the present study, peroxisome-enriched fractions (PEFs) from Sendai virus (SeV)-infected or uninfected HepG2 cells were obtained and subjected to quantitative proteomics analysis. We identified 311 proteins that were significantly changed by SeV infection. Among these altered proteins, 25 are immune response-related proteins. Further bioinformatic analysis indicated that SeV infection inhibits cell cycle-related proteins and membrane attack complex (MAC)-related proteins, all of which are beneficial for the survival and replication of SeV within host cells. Using Luciferase reporter assays on several innate immune-related reporters, we performed functional analysis on 11 candidate proteins. We identified LGALS3BP and CALU as potential negative regulators of the virus-induced activation of the type I interferons (IFNs).

Keyword: Sendai virus (SeV), dimethylation, quantitative proteomics, interferon signaling, innate immunity, CALU, LGALS3BP

Introduction

One of the most significant evolutionary features in eukaryotes is the appearance of a membrane system to separate enzymatic reactions and to provide scaffolds for signal transduction. The small genome of viruses requires that they use the host's cellular machinery, especially host intracellular membranes, to assemble their replication complexes and to complete their replication cycle (1). Therefore, it is not surprising to find that the eukaryotic membrane system is also involved in antiviral responses (2-4).

Subcellular organelles with extensive membrane systems include the endoplasmic reticulum (ER), mitochondria, endosomes and peroxisomes. Despite their well-recognized functions in cell metabolism, these organelles and their related membranes have been identified in recent years as important innate immune platforms (5). The ER is a key organelle for maintaining cellular homeostasis. Several recent studies have linked the ER to antiviral immune responses and have elucidated the related mechanisms (6-10). The mitochondria serve mainly as the power plants of eukaryotic cells but also participate in numerous crucial cellular processes, such as calcium homeostasis, apoptosis and aging (11-13). In recent years, the mitochondria and mitochondrial-associated membranes (MAM) have also emerged as fundamental hubs for innate antiviral immunity. Several important antiviral immune-related proteins, such as VISA (also referred to as MAVS/CARDIF/IPS-1) and MITA (also referred to as STING), have been found to localize to the mitochondrial membrane (14-19). Peroxisomes are monolayer-membrane organelles present in nearly all types of human cells, with a particularly high abundance in hepatocytes and nephrocytes, which are involved in various oxidative enzymatic reactions. It has been reported that the peroxisomal-associated protein VISA induces a rapid interferon (IFN)-independent expression that provides short-term protection, whereas the mitochondrial-associated VISA activates an IFN-dependent signaling pathway with delayed kinetics (20). The peroxisomal VISA can activates IRF1-mediated IFN-λ production (21). The endosomes, although known as players in cellular endocytosis and vascular transport, have functions that extend to the antigen presentation of major histocompatibility complex (MHC) class I,

MHC class II and CD1 molecules of the adaptive immune system, as well as pattern recognition of innate immune-related receptors, such as Toll-like receptors (TLRs) and NOD-like receptors (NLRs) (22, 23).

Subcellular fractionation is an effective experimental strategy for isolating/enriching specific organelles. Compared to whole-cell-based proteomic analysis, combining the isolation of subcellular components with mass spectrometry-based proteomic analysis is advantageous not only for characterizing low abundance proteins but also for monitoring protein abundance changes at the organelle level. To systematically analyze the role of peroxisomal-related proteins in innate immune responses, we used a modified two-step gradient centrifugation method to enrich the peroxisomes from cells with or without SeV infection, followed by a quantitative proteomic analysis. A total of 2946 proteins were quantified among which 311 proteins were found to be significantly changed by SeV infection. A statistical enrichment test was used to reveal that 13 protein groups were changed significantly ($p < 0.05$) compared to the entire protein list. Cell cycle-related proteins and membrane attack complex (MAC)-related proteins were down-regulated, which may facilitate virus survival and replication in host cells. Luciferase reporter assays were performed to further screen for the significantly changed proteins that could affect SeV-induced activation of the type I IFN signaling pathway. Not only does our data provide new and unbiased protein-level information regarding viral infection processes, we also provide direct evidence for the involvement of two proteins (CALU and LGALS3BP) as potential negative regulators in the virus-triggered induction of the type I IFNs.

Material and methods:

Reagents and antibodies

Chemical and cell-culture reagents: DMEM (Thermo, USA), FBS (Gibco, USA), Milli-Q-quality water, HPLC-grade methanol (Tedia, USA), trifluoroacetic acid (TFA, Sigma, USA), acetonitrile (Tedia, USA), ammonium formate (Fluka, USA), formic acid (Fluka, USA), ammonium hydroxide (Fluka, USA),

Nycodenz (Axis-Shield, Norway), and protease inhibitor mixture cocktail tablets (Roche, USA). Other unspecified reagents were obtained from Sigma.

Cell culture and preparation of the peroxisome-enriched fraction

HepG2 cells were cultured in DMEM media and 10% FBS. The cells (5×10^8) were infected with SeV at a multiplicity of infection (MOI) of 100 for 12 hours, with mock-infected cells as controls. The cells were harvested in PBS solution and homogenized in HM buffer (5 mM MOPS, 1 mM EDTA-Na, 250 mM sucrose, 0.1% ethanol, pH 7.2) using a 7-ml volume homogenizer (Sigma, USA) on ice. Trypan blue was used to monitor the break rate of the cells. When the cell break rate reached 80% - 85%, the cell homogenization was considered to be complete.

The peroxisome-enriched fractions (PEFs) were prepared using a published two-step gradient centrifugation protocol with modifications (24). The cell homogenates were centrifuged at 800 × g for 10 minutes. The supernatant was collected and centrifuged at 6,000 × g for 10 minutes. Then, the supernatant was centrifuged at 20,000 × g for 15 minutes in a SW40 rotor (Beckman). The sediment, which is generally recognized as the light mitochondrion-containing fraction, was then gently homogenized in HM buffer (0.25 M sucrose, 5 mM MOPS, 1 mM EDTA-Na, 0.1% ethanol, pH 7.2, with protease inhibitor cocktail). The continuous density gradient was prepared using Nycodenz, which is a nonionic iodinated density gradient medium. It is widely used for the isolation of cells, subcellular organelles and membranes, macromolecules and viruses (25). A 10% (W/V) Nycodenz solution was prepared in HM buffer, and a 40% Nycodenz solution was prepared in HD buffer (5 mM MOPS, 1 mM EDTA-Na, 0.1% ethanol, pH 7.4). Finally, a 9-ml 10-40% (W/V) Nycodenz continuous density gradient (density span from 1.05 to 1.21 g/ml) was made using a double-chamber mixture. The centrifugation was performed at 170,000 × g for 150 minutes at 4°C. After the centrifugation, fractions of 0.5-ml each were collected and analyzed via western blot using PMP70 and AIF as protein markers to indicate the peroxisome and

mitochondrial locations. Generally, from the highest to the lowest density fractions, PMP70-(peroxisome marker) staining appears first, without any AIF-staining. After three fractions, the AIF-staining appears, and overlaps with the PMP70-staining for another 8-10 fractions. Because mitochondrial proteins are generally in greater abundance than peroxisomal proteins, to ensure the maximum removal of the mitochondrial proteins, only the first three PMP70-stained fractions were combined and used in this proteomic analysis.

Protein isolation, digestion, and labeling with dimethylation reagents

Three volumes of HD buffer were added to each fraction and centrifuged at 22,000 × g for 30 minutes. The sediment was lysed with 1% (W/V) sodium carbonate solution, and the lysate was then mixed with 3 volumes of protein precipitation solution (50% acetone, 50% methanol and 0.1% acetic acid) and placed at -20°C for 2 hours, then centrifuged at 2000 × g for 20 minutes. The protein pellets were resuspended in a buffer containing 8 M urea, 4 mM $CaCl_2$, and 0.2 M Tris-HCl, pH 8.0. The proteins were reduced with DTT, alkylated with iodoacetamide, and then digested with trypsin as previously described (26). The digested peptides were desalted with a SepPak C18 cartridge (Waters, USA), dried in a SpeedVac, dimethyl-labeled with either CH_2O (light labeled, the SeV-stimulated sample) or CD_2O (heavy labeled, the mock control sample). The dimethyl-labeling experiment was performed following by a previously reported protocol (27). The light- and heavy-labeled peptides were mixed at a ratio of 1:1 and separated using strong cation exchange (SCX) chromatography into 10 fractions, as previously described (26). Each fraction was desalted using a ZipTipC18 micropipette tip (Millipore, USA), dried with a SpeedVac, and stored at -80°C before the LC-MS/MS analysis.

Mass spectrometry analysis and data processing

The protein samples from three biological replications were generated and analyzed independently. Using SCX fractionation, each sample group was separated into 10 fractions, followed by analytical LC-MS/MS runs. A TripleTOF 5600+ System coupled with an Ultra 1D Plus nano-liquid chromatography device (AB SCIEX, USA) was used for tandem mass spectrometry analysis. Peptides were dissolved in 2% acetonitrile and 0.1% formic acid, loaded onto a C18 trap column (5 μm, 5 × 0.3 mm, Agilent) at a flow rate of 5 μL/min, and subsequently eluted from the trap column over the C18 analytic column (75 μm × 150 mm, 3 μm particle size, 100 Å pore size, Eksigent) at a flow rate of 300 nL/min in a 100 min gradient. The mobile phase A was 3% DMSO and 0.1% formic acid, the mobile phase B was 3% DMSO, 97% acetonitrile and 0.1% formic acid. The information dependent acquisition (IDA) mode was used to acquire MS/MS data. Survey scans were acquired in 250 ms and 40 product ion scans were collected at 50 ms/per scan. The precursor ion range was set from m/z 350 to m/z 1500, and the product ion range was set from m/z 100 to m/z 1500. Tandem mass spectra were extracted by Peakview version 2.0 (AB SCIEX, USA).

Analysis of the raw MS spectra was performed with Proteinpilot 5.0 software (AB SCIEX, USA) using the Paragon algorithm. The uniprot_2014_8 database (Proteome ID: UP000005640, downloaded in Aug, 2014) was used, and the data analysis parameters were as follows: Sample type: Dimethyl +0, +4 (Peptide Labeled); Cys Alkylation: Iodoacetamide; Miss cleavages tolerance: 2; Digestion: Trypsin; Fixed modification: carbamidomethyl Cys; Variable modification: none; Special Factors: Urea denaturation; MS1 initial mass error tolerance value: 0.05 dalton; MS2 initial mass error tolerance value: 0.1 dalton. Three independent biological replicates were generated and analyzed. The false discovery rates (FDRs) of Proteinpilot search results were all set as lower than 1% at the protein level. The protein ratios used for relative quantitation were calculated as previously described (28). The confidence of each quantitative peptides higher than 99% were picked up. In each replicates, there are at least two or more unique quantitative peptides for each proteins' quantification. The protein ratio values used in the bioinformatics analysis described below are the means of the three biological replicates.

Before bioinformatics analysis, the thresholds of "significantly-changed" ratios were calculated. Based on the Gaussian distribution of the quantitative ratio (log_2 value) list, the mean and the standard deviations value of the Gaussian distribution were calculated as previously described method (29).

To identify specific protein categories that are significantly affected by viral infection, the "statistical overrepresentation test" and "the statistical enrichment test" tools in PANTHER classification system (http://www.pantherdb.org, version 9.0) was used. Gene Ontology (http://www.geneontology.org, version 2.44), KEGG database (http://www.kegg.jp, release Dec, 2014) and DAVID functional annotation tools (http://david.abcc.ncifcrf.gov, version 6.7) were also used to analyze the data.

Transfection and reporter assays

The cells were seeded and transfected the following day using a standard calcium phosphate precipitation method or via FuGENE (Roche). Empty control plasmids were added to ensure that each transfection received the same amount of total DNA. To normalize the transfection efficiency, pRL-TK Renilla luciferase reporter plasmids were added to each transfection. The luciferase assays were performed using a Dual-Specific Luciferase Assay kit (Promega), in which the firefly luciferase activities were normalized on the basis of the Renilla luciferase activities.

RNAi experiments

The single-stranded siRNA corresponding to the target gene sequences were based on the Sigma siRNA library. The following siRNA sequences were used: For human CALU: #1: 5′-GUUAGAGAUGAGCGGAGGUUU-3′; #2: 5′-CGUUGACAAGUAUGACUUAUU-3′. For human LGALS3BP: #1: 5′-GAGCGCUCAGCUUCAAGAAAU-3′; #2: 5′-UGUGGUCUGCACCAAUGAAAC-3′.

Western blot

Proteins separation by SDS-PAGE (10% gel) and western blotting were performed as previously described (30). The following antibodies were used in the experiments: mouse monoclonal anti-AIF (Santa Cruz, Cat. # sc-55519); mouse monoclonal anti-PMP70 (Invitrogen, Cat. # 718300); rabbit polyclonal anti-CALU (Santa Cruz, Cat. # sc-98983); rabbit polyclonal anti-LGALS3BP (Santa Cruz, Cat. # sc-98706); mouse monoclonal Anti-HA (Sigma, Cat. # H9658).

ELISA

The supernatants of cell culture medium were analyzed with a human IFN-β ELISA kit (PBL Assay Science) following protocols recommended by the manufacturer.

Results

Experimental design and overview of the quantitative proteomic data

HepG2 is a widely used human liver cell line. Because of their high degree of morphological and functional differentiation in vitro, HepG2 cells are also widely used in studies of intracellular protein trafficking (31, 32). Previous studies have shown that in HepG2 cells, two of the most important innate immune pathways, the RLRs and TLRs signal pathways, can be activated after viral infection (33, 34). To establish a proper cell stimulation condition for our proteomic study, we stimulated HepG2 cells with SeV at an MOI of 100 for 12 hours and then validated SeV-induced activation of IFN-β, ISRE and NF-κB using luciferase reporter assays (data not shown).

Our subcellular and quantitative proteomic analysis workflow is outlined in Figure 1A. HepG2 cells, with or without SeV infection, were obtained, and the PEFs (35) were isolated using a two-step Nycodenz gradient centrifugation as described in the methods section. After obtaining the PEFs, the proteins were digested with trypsin followed by peptide-level stable isotope dimethylation. The SeV-infected sample was labeled with the "heavy" reagent, while the mock treated sample was labeled with the "light" reagent. Dimethyl labeled peptides were mixed at a 1:1 ratio, fractionated into 10 fractions via SCX, and then analyzed using LC-MS/MS analysis (Fig. 1A).

Three biological replicates were generated and analyzed independently using the workflow outlined in Figure 1A. Overall, 3735, 3675 and 3879 non-redundant proteins were identified from the three biological replicates (FDR < 1%) (Table S1). A total of 42760, 44065 and 42275 quantified peptides passed the stringent quality test in replicates 1, 2 and 3, respectively (Table S2). There are at least two or more unique quantitative peptides for each proteins' quantification. And finally 2317, 2359 and 2364 proteins were quantified in three replicates, respectively (Table S3). When the quantified proteins from the three biological repeats were combined, 1771 proteins were found to be in common, and a total of 2946 non redundant proteins were quantified in these three replicates (Table S3). A data correlation analysis of the 1771 proteins showed the Pearson correlation coefficient values of 0.787, 0.587 and 0.632, respectively among the replicates (Fig. 1B).

To define the "significantly changed" proteins, we analyzed the Gaussian distribution of the quantitative ratio (as $\log_2$ value) (Fig. 1C), and calculated the mean and the SD (standard deviation) value of the Gaussian distribution. If setting the mean ± 1.96SD as significantly changed threshold, the up-regulated quantitative ratio cutoff was 1.542 and the down-regulated quantitative ratio cutoff was 0.654, respectively. Based on these threshold values, there were 99 up-regulated and 212 down-regulated proteins (see full regulated protein list in Table S3).

Because we conducted a subcellular proteomic study, not a whole-cell-based study, it is important to find certain organelle protein markers, especially those that are highly abundant, and housekeeping

protein markers, which are among the groups of unchanged proteins, to serve as reference controls, as this proves that the subcellular fractionation method itself did not introduce biased data. Indeed, many organelle protein markers were found to be unchanged, including two peroxisome proteins, peroxisome assembly factor PEX6 (average ratio = 1.019) and peroxisome biogenesis factor PEX1 (average ratio = 0.945), the ER-located protein fatty aldehyde dehydrogenase AL3A2 (average ratio = 1.09), the ER membrane protein complex subunit EMC1 (average ratio = 1.105), the mitochondrially located ATP synthase subunit beta ATPB (average ratio = 1.032) and malate dehydrogenase MDHM (average ratio = 1.022).

Bioinformatic analysis of the regulated proteins

We also analyzed the subcellular localization information for all of the quantified proteins by Gene Ontology (Table S4). Among the 2946 quantified proteins, 2687 proteins have cellular component information in the GO database. Among the 99 up- and 212 down-regulated proteins, 90 and 193 proteins have cellular component information, respectively. The protein distribution in each subcellular location is shown in Figure 1D (details in Table S4). Because some proteins may have information on more than one subcellular location in the GO database, the sum of all of the ratios may be greater than 100%. As an evidence for the peroxisome enrichment, the Fisher exact P-value, a value measures the subcellular gene-enrichment in the DAVID annotation system (36), was calculated as 6.61 E^{-20} (Table S4).

Although we employed a two-step Nycodenz gradient centrifugation strategy to enrich the peroxisomes, many proteins from other subcellular localizations, in particular, the ER (15.22%), Golgi apparatus (8.48%) and mitochondria (17.79%), were also present, which is likely due to the similar cellular densities of these organelles with peroxisomes (Fig. 1D). Upon comparing the protein distributions of all of the proteins identified among the up- or the down-regulated proteins (Fig. 1D), we found that the up-regulated proteins were disproportionally overrepresented in the lysosome (12.22% of

the up-regulated proteins vs 2.42% of the total) and endosome (5.55% of the up-regulated proteins vs 3.20% of the total), while the overrepresented proteins in the down-regulated groups included the cytoskeleton (8.29% of the down-regulated proteins vs 4.09% of the total) and the peroxisome-related proteins (4.14% of the down regulated proteins vs 2.31% of the total). The up-regulated lysosome and endosome proteins (Table S5) are primarily proteins related to immune responses, especially positive regulation of anti-virus defense response, suggesting that the anti-virus defense response activities were enhanced by SeV infection. The down-regulated cytoskeletal-related proteins primarily consisted of myosin and actin cytoskeleton organization related proteins, while the down-regulated peroxisomal proteins were found to be primarily involved in lipid metabolism.

To further define the altered proteins by function, we used the PANTHER "statistical enrichment test" tool to determine whether a certain protein class is significantly changed with respect to the entire list of quantitative proteins (37). According to the biological process classification, the up-regulated biological processes were protein localization to ER (p = 4.56 E^{-5}), viral life cycle (p = 1.15 E^{-3}), extracellular structure (p = 1.09 E^{-2}), and viral transcription (p = 4.91 E^{-2}) (Fig. 2A-D). And the down-regulated biological processes were cell cycle process (p = 3.12 E^{-6}), microtubule-based process (p = 2.20 E^{-3}), mRNA processing (p = 6.06 E^{-3}), and peroxisome organization (p = 3.62 E^{-2}) (Fig. 2E-H). As housekeeping/unchanged control groups, the catabolic process proteins and the biosynthetic process protein groups were not significantly changed. According to the molecular function classification, the up-regulated molecular function groups were oxidoreductase activity (p = 3.68 E^{-2}), clathrin binding (p = 1.26 E^{-2}) (Fig. 3A, 3B). And the down-regulated molecular function groups were motor activity (p = 2.49 E^{-2}), nucleotide binding (p = 4.13 E^{-5}), and small molecular binding (p = 7.09 E^{-4}) (Fig.3C-E). As the housekeeping/unchanged control groups here, the structural molecule activity protein and the hydrolase activity protein groups were not significantly changed.

Putting the abundant "un-changed" proteins aside, by combining the information from the PANTHER "statistical overrepresentation test", KEGG pathway analysis and UniProt annotations, we

grouped the significantly changed proteins together based on their functions and found that proteins within a functional group mostly have the same regulatory trend (Fig. 4, Table S6). Many of these altered proteins are known to have activities in the host cell's anti-viral response. Among the up-regulated proteins, two groups, "immune response" and "antigen processing and presentation", stood out (Fig. 4). In the immune response group, ZCCHV is a known antiviral protein that inhibits the replication of viruses by recruiting cellular RNA degradation machinery to degrade viral mRNAs (38). IFM1 is an IFN-induced antiviral protein which inhibits the entry and replication of viruses to the host cell cytoplasm (39, 40). IFM3 is a IFN-induced antiviral protein which could disrupts intracellular cholesterol homeostasis, thus inhibits the entry of viruses to the host cell cytoplasm by preventing viral fusion with cholesterol depleted endosomes(41, 42). OSAL could against encephalomyocarditis virus (EMCV) and hepatitis C virus (HCV) via an alternative antiviral pathway independent of RNase L (43, 44). PLS1 may play a role in the antiviral response of IFNs by amplifying and enhancing the IFN response through increased expression of select subset of potent antiviral genes (45). IF16 Involved in innate immune response by recognizing viral dsDNA in the cytosol, after binding to viral DNA recruits TMEM173/MITA and mediates the induction of IFN-β (46). In the antigen processing and presentation group, AP2A1, AP2A2, AP2B1 AP2M1, and AP2M1 all are components of the adaptor protein complex 2 (AP-2), which functions in protein transport via the transport of vesicles through different membrane traffic pathways (47, 48). The AP-2 complex is involved in antigen processing and the presentation of exogenous antigens via MHC class II (49). Additionally, TAP1 and TAP2 form the TAP complex, which mediate the MHC class I antigen processing and the presentation processes (50).

Among the down-regulated proteins, four protein groups stood out: membrane attack complex (MAC)-related proteins, cytoskeletal proteins, cell cycle-related proteins and negative regulation of antiviral response proteins (Fig. 4). There were 7 MAC constitute proteins (CO3, CO4A, CO5, CO6, CO7, CO8B and CO9) which were significantly down-regulated. MAC plays a key role in the innate and adaptive immune response by forming pores in the plasma membrane of target cells (51). Inflammatory

responses can be triggered by MAC. And a sublytic MAC attack can increase the cytosolic Ca^{2+} concentration and ultimately lead to inflammation and apoptosis (52). We found a large group of cytoskeletal-, myosin-, and actin organization-related proteins that were down-regulated. Additionally, a set of cell cycle-related proteins were down-regulated. Interestingly, we also found three down-regulated proteins which are known as negative regulators in antiviral responses (Fig. 4). NCBP2 is a component of the cap-binding complex, which involved in pre-mRNA splicing (53). NCBP2 could help viruses replicate in host cells (54). MUL1 negatively regulates innate immune defense against viruses by inhibiting DDX58-dependent antiviral response (55). DNJA3 negatively regulates NF-κB activation (56).

CALU and LGALS3BP negatively regulate SeV-induced activation of IFN-β

The above quantitative proteomic analysis identified 311 proteins that were altered in response to SeV infection. To investigate whether these altered proteins participate in host antiviral innate immune responses, proteins that fit the following requirements were selected for further functional studies: 1) Protein quantification data appears in all three replicates, and had the same trend of regulation. 2) The candidate protein function was unknown or its previous reported function was unrelated to host immune responses. 3) The human cDNA expression plasmid is readily available in an Origene cDNA library. By following the above criteria, 11 candidates were selected and tested for their potential effect in SeV-induced IFN-β, ISRE, NF-κB and IFN-γ-induced IRF-1 activation. These 11 candidates are PDLIM5, CALU, CSRP1, PDIA6, GNPAT, LGALS3BP, PEX11B, EHHADH, HMGA1, PEX16 and GNB2.

Viral induced IFN-β, ISRE, NF-κB and IFN-γ-induced IRF-1 activation are well established assays for the study of innate immunity (14, 57). The strength of a cell's antiviral abilities can be monitored by the relative activation level of IFN-β, ISRE and NF-κB reporters upon viral infection. IFN-β, a cytokine in the type I IFN family, is involved primarily in the antiviral innate immune response. NF-κB is a protein complex that controls the transcription of DNA in response to multiple stimuli, such as stress, cytokines

and bacterial or viral antigens. Activated NF-κB binds to κB and the IFN-stimulated response element (ISRE) enhancer motif of the IFN-β promoter, leading to transcriptional induction of the IFN-β gene (58). IFN-γ belongs to the type II IFN family and can induce IRF1 activity (59). IRF-1 reporter was used in this research as a control reporter to identify the specificity of the signal pathway.

In an initial screening experiment, human cDNA over-expression plasmids for the 11 selected candidate genes were tested for their ability to influence SeV-induced IFN-β, ISRE and NF-κB reporters activation, and IFN-γ induced IRF-1 reporter activation via reporter assays (Fig. 5A-5D). Over-expression of three candidates (*CALU, LGALS3BP* and *EHHADH*) showed negative effects on SeV-induced IFN-β, ISRE and NF-κB reporter activities, while the overexpressed *PEX16* cDNA showed a positive effect on NF-κB reporter activity.

To further define the roles of the 4 candidate proteins in the regulation of SeV-induced type I IFN signaling pathways, 4 over-expression plasmids were transfected into 293 cells at different dosages. Their abilities to affect SeV-induced activation of the IFN-β, ISRE and NF-κB reporters and the IFN-γ induced IRF-1 reporters were tested using luciferase reporter assays. Overexpression of either CALU or LGALS3BP inhibited SeV-induced activation of IFN-β, ISRE and the NF-κB reporter in a dose-dependent manner (Fig. 6A, 6B), and an increased dosage barely affected the IFN-γ-induced activation of the IRF-1 reporter (Fig. 6C, 6D). Overexpression of EHHADH inhibited SeV-induced IFN-β and the NF-κB reporter activity but also enhanced SeV-induced ISRE reporter activity in a dose-dependent manner (Fig. 6E). Overexpression of PEX16 potentiated SeV-induced ISRE and IFN-β reporter activity in a dose-dependent manner but barely affected SeV-induced NF-κB reporter activity (Fig. 6F). As EHHADH and PEX16 were also able to activate the IFN-γ-induced activation of the IRF-1 reporter, and over-expression of PEX16 activated NF-κB reporter without stimulation. (Fig. 6G, 6H, 6F), we speculated that EHHADH and PEX16 may not be specifically involved in SeV-activated IFN-β induction. These data however, suggest that CALU and LGALS3BP are specifically involved in SeV-induced activation of IFN-β.

To further validate the potential effect of CALU and LGALS3BP on SeV-induced activation of IFN-β production, two sets of siRNAs targeting different sites in human *CALU* and *LGALS3BP* mRNA were generated, respectively. The knockdown efficiency of these siRNAs targeting *CALU* or *LGALS3BP* mRNA were more than 50% (Fig. 6A, 6B). Western blot analysis also shown that these two sets of siRNAs could significantly inhibit CALU and LGALS3BP proteins expression, respectively (Fig. 6C, 6D). Reporter assays indicated that knockdown of CALU or LGALS3BP potentiated SeV-induced activation of the IFN-β, ISRE and NF-κB reporters and barely affected the IFN-γ-induced activation of the IRF-1 reporter (Fig. 6E-H). Additionally, knockdown of CALU or LGALS3BP potentiated SeV-induced transcription of the *IFNB1* gene and SeV-induced IFN-β protein levels (Fig. 6A, 6B). These results collectively prove that CALU and LGALS3BP act as potential negative regulators in virus-triggered type I IFN signaling.

Discussion

HepG2 is a well-differentiated hepatocellular carcinoma cell line. Because HepG2 cells have a well-established intracellular membrane trafficking system, they are widely used as cultured cells for the extraction of peroxisomes, lysosomes and endosomal subcellular organelles (60-62). This phenomenon is also the reason why we chose HepG2 as the host cell for our study focusing on viral-induced alterations in peroxisome-associated proteins. The SeV infection conditions, the MOI and the infection time were primarily based on our previous studies (30), to ensure that the proteomic data could be compared with those studies.

We first eliminated the nuclear and heavier mitochondria to obtain the so-called “light mitochondrial fraction” (LMF) (63), in which the peroxisomes are heavier than the ER, Golgi apparatus membrane, lysosome, mitochondrion in LMF with a density range of 1.17-1.20 g/ml in Nycodenz (64). To ensure the maximum enrichment of the peroxisomes and the peroxisome-associated membranes, following a

gradient centrifugation, we avoided any fractions where the peroxisomes and mitochondria overlapped. Based on the identified proteins, in addition to the peroxisome proteins, our subcellular fractionation method was also enriched for proteins localized in the ER and Golgi apparatus but effectively eliminated the highly abundant nuclear and cytosolic proteins. The important innate immune adaptor VISA was also found in the PEFs, which coordinate with the previous studies (20, 21). Compared to whole-cell based proteomic analysis, the organelle proteomic approach has certain advantages. First, it decreases the complexity of the samples to be analyzed, thus increasing the chance of identifying less abundant proteins. Second, the protein quantitation information that is obtained is organelle specific; therefore, the protein relocalization or movement-related information can be captured.

For years, studies on peroxisomes have focusing primarily on the catabolism of very-long-chain fatty acids, branched chain fatty acids, D-amino acids, and polyamines, as well as the biosynthesis of phospholipids critical for the normal function of mammalian brains and lungs (65). Our current study represents the first proteomics-based analysis that specifically focuses on peroxisome-related proteins in the innate immune response to a virus. We identified 311 proteins in the PEFs that showed alterations following the SeV infection. Among the 311 proteins, 25 proteins have been linked to human immune response-related processes. One of the key discoveries from our quantitative proteomic study is that SeV infections affect the host cell cycle and membrane attacking processes. A bioinformatics analysis revealed that many cell cycle-related proteins were down-regulated upon SeV infection, especially the spindlin complex organization-related proteins (Fig. 4). Many viruses, including DNA, retro, and RNA viruses can affect the cell cycle processes in order to increase the efficiency of virus replication (66). In the DNA viruses, the simian virus (SIV) E1A protein and papillomavirus (HPV) E7 protein can interact with cellular retinoblastoma protein (pRB) to release the transcription factor E2F. Release of E2F permits a set of gene transcriptions which are necessary for the DNA replication and cell proliferation, thus promotes host cell into S phase (67, 68). Simian virus SV5 protein can slow the progression of the cell cycle (69). Herpes simplex virus (HSV) can block pRB phosphorylation to inhibit cell progression from G1 to S

phase (70). Human cytomegalovirus (CMV) UL69 protein inhibits cell progression from G1 to S phase (71). Retro virus like human immunodeficiency virus (HIV) Vpr protein can prevent cyclin B/cdc2 activation causing cell accumulation in G2-M phase (72). Compare to DNA virus, less is known about how RNA viruses regulate with host cell cycle. Hepatitis C Virus (HCV) infection causes cell cycle arrest at the interface of G2 and mitosis (73). Measles virus (MeV) causes G1 arrest in virus-infected T lymphocytes (74). We speculate that the down-regulation of mitotic cell cycle-related proteins we observed in this study may also part of the host response to virus replication. Additionally, we found that the MAC-related proteins were down regulated, this links the SeV infection to inflammation and the apoptosis response (52).

The host cell's cytoskeletal system is closely tied to viral infection and replication. Viruses not only use cytoplasmic membrane trafficking but also the cytoskeletal transport machinery to facilitate their intracellular transport (75). We found that many of the cytoskeletal-related proteins were down-regulated following SeV infection in the PEFs, including 8 myosin subunits and 5 actin polymerization regulators (Table S6). Myosins comprise a family of ATP-dependent motor proteins, which can interact with actin filaments to form stress fibers (76). Previous studies showed that the disruption of the normal function of myosin 2 by inhibitors can disturb the entry and budding of HIV (77, 78). The small GTPase RRAS regulates the organization of actin and drives membrane protrusions (79). GMIP stimulates the GTPase activity of RhoA (80). And MRCKA is a downstream effector of CDC42, which regulates actin cytoskeletal reorganization via phosphorylation of PPP1R12C and MYL9/MLC2 (81). Actin polymerization is closely tied to viral infection processes (75). The intact actin cytoskeleton structure is crucial for proper activation of antiviral response (82). Previous quantitative proteomic studies of viral-infected host cells found that the cytoskeletal proteins are also downregulated by transmissible gastroenteritis virus (TGEV), infectious bursal disease virus (IBDV) and porcine circovirus type 2 (PCV2) infection (83-85). Although our fractionation quantitative proteomics could not directly reflect the total amount of host-cell proteins, the regulated proteins are actually influenced by the SeV infection. An et al.

speculated that the actin cytoskeletal network collapses and disperses, leading to an unstable cytoskeletal structure, thus facilitating the release of TGEV particles from the host cells (83). We believe that it is possible that the disruption of the host cell's cytoskeletal network may facilitate the budding of viral particles. However, the precise mechanism of how the down-regulated cytoskeletal network affects the viral replication process is still unknown.

Through reporter assays, we screened for proteins that played a role in SeV-induced activation of IFN-β. Four proteins (CALU, LGALS3BP, EHHADH and PEX16) that are potentially involved in virus-triggered type I IFN signaling were identified. Using dose-dependent overexpression and RNAi assays, we confirmed that CALU and LGALS3BP act as potential negative regulators in virus-triggered type I IFN signaling. Calumenin (CALU), a calcium ion binding protein found in the ER and in the melanosomes (86, 87), is involved in the regulation of the vitamin K-dependent carboxylation of multiple N-terminal glutamate residues. CALU has been reported to be a secreted protein, but the secretory process and the regulatory mechanism are largely unknown (88). Lectin galactoside-binding soluble 3 binding protein (LGALS3BP) is a glycosylated secreted molecule that has previously been shown to be associated with the development of metastases in a variety of human cancers (89-92). Previous studies indicated that LGALS3BP may stimulate the host's defense against viruses and tumor cells (93). The infection of human muscle satellite cells by the dengue virus (DENV) leads to the elevation of LGALS3BP protein levels (94). The quantitative proteomic analysis indicated that CALU and LGALS3BP were up-regulated in the PEFs upon SeV infection, but the mRNA levels of the proteins were not significantly regulated following the SeV infection (Fig. 7A, 7B). Therefore, we believe that the SeV infection may induce the transport of CALU and LGALS3BP to the secretory apparatus, thus transporting them into the extracellular space. However, the precise mechanism of how these proteins regulate host cell immune responses needs more evidences.

Peroxisomal bifunctional enzyme EHHADH is a β-oxidation enzyme which generates hydrogen peroxide required for peroxisomal biogenesis and lipid metabolism. This enzyme may involve in the

leukaemia disease and leukoencephalopathy disease (95, 96). Increased EHHADH activity has been seen in some acute leukaemia and human carcinoma patients (97, 98). The enzyme activity can be enhanced by acetylation (99). Peroxisomal membrane protein PEX16 may play a role in early stages of peroxisome assembly, can function as receptor for PEX3, to de novo peroxisomes derived from the ER (100-102). EHHADH and PEX16 can enhance the IFN-γ-induced activation of the IRF-1 reporter (Fig. 6G, 6H). We speculate that these two proteins may involve in other immune signaling pathways.

For conclusion, our study represents the first quantitative proteomics-based analysis that specifically focuses on peroxisome-related proteins in the innate immune response to a virus. We identified 311 proteins that are significantly changed by SeV infection. We found that SeV infection inhibits cell cycle-related proteins and membrane attack complex (MAC)-related proteins, all of which are beneficial for the survival and replication of SeV within host cells. Using luciferase reporter assays on several innate immune-related reporters, we identified LGALS3BP and CALU as potential negative regulators of the virus-induced activation of the type I IFNs.

Supporting Information

Supplementary Table S1: Overview of the protein and peptide identification results. There are a total of 6 sheets: the protein and peptide identification data for the first, second and third biological repeat.

Supplementary Table S2: Overview of the peptide quantitative results. There are a total of 3 sheets: the peptide quantification data for the first, second and third biological repeat.

Supplementary Table S3: Overview of the protein quantitative results. There are a total of 7 sheets: the protein quantification data for the first, second and third biological repeat, the protein quantification data for the common proteins in the three repeats, the total non-redundant quantified proteins in the three repeats, the up-regulated proteins and the down-regulated proteins.

Supplementary Table S4: The subcellular localization information of the total quantified proteins, the up-regulated proteins and the down-regulated proteins. There are a total of 3 sheets: the subcellular localization information for all of the quantified proteins, up-regulated proteins and down-regulated proteins generated by Gene Ontology.

Supplementary Table S5: The PANTHER statistical enrichment test. There are a total of 6 sheets: the PANTHER enrichment test by GO biological process categorization, the detailed protein list of biological process, the PANTHER enrichment test by GO molecular function categorization, the detailed protein list of molecular function, the PANTHER enrichment test by PANTHER protein class categorization and the detailed protein list of PANTHER protein class.

Supplementary Table S6: The functional categorization of the regulated proteins.

Supplementary spectra S7: Annotated spectra for all single peptide identifications in the three biological replicates.

Author Information

Correspondence Authors

Dr. Hong-Bing Shu; Email: shuh@whu.edu.cn; Tel: +86-27-68753795

Dr. Lin Guo; E-mail: guol@whu.edu.cn; Tel: +86-27-68753800

Acknowledgements

We would like to thank Yong Zhao for assistance in the proteomic analysis. This work was supported by grants from the National Basic Research Program of China (#2013CB911102), the Natural Science Foundation of China (NSFC #31221061), and the 111 Project of China (B06018) to Wuhan University.

References

1. Salonen, A., Ahola, T., and Kaariainen, L. (2005) Viral RNA replication in association with cellular membranes. *Current topics in microbiology and immunology* 285, 139-173
2. Pestka, S., Krause, C. D., and Walter, M. R. (2004) Interferons, interferon-like cytokines, and their receptors. *Immunological reviews* 202, 8-32
3. Stark, G. R., Kerr, I. M., Williams, B. R., Silverman, R. H., and Schreiber, R. D. (1998) How cells respond to interferons. *Annual review of biochemistry* 67, 227-264
4. Taniguchi, T., Fujii-Kuriyama, Y., and Muramatsu, M. (1980) Molecular cloning of human interferon cDNA. *Proceedings of the National Academy of Sciences of the United States of America* 77, 4003-4006
5. Kagan, J. C. (2012) Signaling organelles of the innate immune system. *Cell* 151, 1168-1178
6. Martinon, F., and Glimcher, L. H. (2011) Regulation of innate immunity by signaling pathways emerging from the endoplasmic reticulum. *Current opinion in immunology* 23, 35-40
7. Colbert, R. A., DeLay, M. L., Klenk, E. I., and Layh-Schmitt, G. (2010) From HLA-B27 to spondyloarthritis: a journey through the ER. *Immunological reviews* 233, 181-202
8. Roy, C. R., Salcedo, S. P., and Gorvel, J. P. (2006) Pathogen-endoplasmic-reticulum interactions: in through the out door. *Nature reviews. Immunology* 6, 136-147
9. He, B. (2006) Viruses, endoplasmic reticulum stress, and interferon responses. *Cell death and differentiation* 13, 393-403
10. Martinon, F. (2012) The endoplasmic reticulum: a sensor of cellular stress that modulates immune responses. *Microbes and infection / Institut Pasteur* 14, 1293-1300
11. Gunter, T. E., Yule, D. I., Gunter, K. K., Eliseev, R. A., and Salter, J. D. (2004) Calcium and mitochondria. *FEBS letters* 567, 96-102
12. Wang, C., and Youle, R. J. (2009) The role of mitochondria in apoptosis*. *Annual review of genetics* 43, 95-118
13. Seo, A. Y., Joseph, A. M., Dutta, D., Hwang, J. C., Aris, J. P., and Leeuwenburgh, C. (2010) New insights into the role of mitochondria in aging: mitochondrial dynamics and more. *Journal of cell science* 123, 2533-2542
14. Xu, L. G., Wang, Y. Y., Han, K. J., Li, L. Y., Zhai, Z., and Shu, H. B. (2005) VISA is an adapter protein required for virus-triggered IFN-beta signaling. *Molecular cell* 19, 727-740
15. Seth, R. B., Sun, L., Ea, C. K., and Chen, Z. J. (2005) Identification and characterization of MAVS, a mitochondrial antiviral signaling protein that activates NF-kappaB and IRF 3. *Cell* 122, 669-682
16. Meylan, E., Curran, J., Hofmann, K., Moradpour, D., Binder, M., Bartenschlager, R., and Tschopp, J. (2005) Cardif is an adaptor protein in the RIG-I antiviral pathway and is targeted by hepatitis C virus. *Nature* 437, 1167-1172
17. Kawai, T., Takahashi, K., Sato, S., Coban, C., Kumar, H., Kato, H., Ishii, K. J., Takeuchi, O., and Akira, S. (2005) IPS-1, an adaptor triggering RIG-I- and Mda5-mediated type I interferon induction. *Nature immunology* 6, 981-988
18. Zhong, B., Yang, Y., Li, S., Wang, Y. Y., Li, Y., Diao, F., Lei, C., He, X., Zhang, L., Tien, P., and Shu, H. B. (2008) The adaptor protein MITA links virus-sensing receptors to IRF3 transcription factor activation. *Immunity* 29, 538-550
19. Ishikawa, H., and Barber, G. N. (2008) STING is an endoplasmic reticulum adaptor that facilitates innate immune signalling. *Nature* 455, 674-678

20. Dixit, E., Boulant, S., Zhang, Y., Lee, A. S., Odendall, C., Shum, B., Hacohen, N., Chen, Z. J., Whelan, S. P., Fransen, M., Nibert, M. L., Superti-Furga, G., and Kagan, J. C. (2010) Peroxisomes are signaling platforms for antiviral innate immunity. *Cell* 141, 668-681
21. Odendall, C., Dixit, E., Stavru, F., Bierne, H., Franz, K. M., Durbin, A. F., Boulant, S., Gehrke, L., Cossart, P., and Kagan, J. C. (2014) Diverse intracellular pathogens activate type III interferon expression from peroxisomes. *Nature immunology* 15, 717-726
22. Bonham, K. S., and Kagan, J. C. (2014) Endosomes as Platforms for NOD-like Receptor Signaling. *Cell Host Microbe* 15, 523-525
23. Gleeson, P. A. (2014) The role of endosomes in innate and adaptive immunity. *Semin Cell Dev Biol* 31, 64-72
24. Ofman, R., Speijer, D., Leen, R., and Wanders, R. J. A. (2006) Proteomic analysis of mouse kidney peroxisomes: identification of RP2p as a peroxisomal nudix hydrolase with acyl-CoA diphosphatase activity. *Biochem J* 393, 537-543
25. Rickwood, D., Ford, T., and Steensgaard, J. (1994) *Centrifugation: essential data*, Wiley
26. Yu, J. L., and Guo, L. (2011) Quantitative proteomic analysis of Salmonella enterica serovar Typhimurium under PhoP/PhoQ activation conditions. *Journal of proteome research* 10, 2992-3002
27. Boersema, P. J., Aye, T. T., van Veen, T. A., Heck, A. J., and Mohammed, S. (2008) Triplex protein quantification based on stable isotope labeling by peptide dimethylation applied to cell and tissue lysates. *Proteomics* 8, 4624-4632
28. Zhang, L. K., Chai, F., Li, H. Y., Xiao, G., and Guo, L. (2013) Identification of host proteins involved in Japanese encephalitis virus infection by quantitative proteomics analysis. *Journal of proteome research* 12, 2666-2678
29. Emmott, E., and Goodfellow, I. (2014) Identification of protein interaction partners in mammalian cells using SILAC-immunoprecipitation quantitative proteomics. *Journal of visualized experiments : JoVE*
30. Qin, Y., Zhou, M. T., Hu, M. M., Hu, Y. H., Zhang, J., Guo, L., Zhong, B., and Shu, H. B. (2014) RNF26 temporally regulates virus-triggered type I interferon induction by two distinct mechanisms. *PLoS pathogens* 10, e1004358
31. Medina-Kauwe, L. K., Xie, J., and Hamm-Alvarez, S. (2005) Intracellular trafficking of nonviral vectors. *Gene therapy* 12, 1734-1751
32. van der Wouden, J. M., van, I. S. C., and Hoekstra, D. (2002) Oncostatin M regulates membrane traffic and stimulates bile canalicular membrane biogenesis in HepG2 cells. *The EMBO journal* 21, 6409-6418
33. Xia, C., Lu, M., Zhang, Z., Meng, Z., Zhang, Z., and Shi, C. (2008) TLRs antiviral effect on hepatitis B virus in HepG2 cells. *Journal of applied microbiology* 105, 1720-1727
34. Israelow, B., Narbus, C. M., Sourisseau, M., and Evans, M. J. (2014) HepG2 cells mount an effective antiviral interferon-lambda based innate immune response to hepatitis C virus infection. *Hepatology* 60, 1170-1179
35. Wolvetang, E. J., Wanders, R. J., Schutgens, R. B., Berden, J. A., and Tager, J. M. (1990) Properties of the ATPase activity associated with peroxisome-enriched fractions from rat liver: comparison with mitochondrial F1F0-ATPase. *Biochimica et biophysica acta* 1035, 6-11
36. Huang da, W., Sherman, B. T., and Lempicki, R. A. (2009) Systematic and integrative analysis of large gene lists using DAVID bioinformatics resources. *Nature protocols* 4, 44-57
37. Mi, H., Muruganujan, A., Casagrande, J. T., and Thomas, P. D. (2013) Large-scale gene function analysis with the PANTHER classification system. *Nature protocols* 8, 1551-1566
38. Kerns, J. A., Emerman, M., and Malik, H. S. (2008) Positive selection and increased antiviral activity associated with the PARP-containing isoform of human zinc-finger antiviral protein. *PLoS genetics* 4, e21

39. Brass, A. L., Huang, I. C., Benita, Y., John, S. P., Krishnan, M. N., Feeley, E. M., Ryan, B. J., Weyer, J. L., van der Weyden, L., Fikrig, E., Adams, D. J., Xavier, R. J., Farzan, M., and Elledge, S. J. (2009) The IFITM proteins mediate cellular resistance to influenza A H1N1 virus, West Nile virus, and dengue virus. *Cell* 139, 1243-1254
40. Raychoudhuri, A., Shrivastava, S., Steele, R., Kim, H., Ray, R., and Ray, R. B. (2011) ISG56 and IFITM1 proteins inhibit hepatitis C virus replication. *Journal of virology* 85, 12881-12889
41. Amini-Bavil-Olyaee, S., Choi, Y. J., Lee, J. H., Shi, M., Huang, I. C., Farzan, M., and Jung, J. U. (2013) The antiviral effector IFITM3 disrupts intracellular cholesterol homeostasis to block viral entry. *Cell Host Microbe* 13, 452-464
42. Feeley, E. M., Sims, J. S., John, S. P., Chin, C. R., Pertel, T., Chen, L. M., Gaiha, G. D., Ryan, B. J., Donis, R. O., Elledge, S. J., and Brass, A. L. (2011) IFITM3 inhibits influenza A virus infection by preventing cytosolic entry. *PLoS pathogens* 7, e1002337
43. Ishibashi, M., Wakita, T., and Esumi, M. (2010) 2',5'-Oligoadenylate synthetase-like gene highly induced by hepatitis C virus infection in human liver is inhibitory to viral replication in vitro. *Biochemical and biophysical research communications* 392, 397-402
44. Marques, J., Anwar, J., Eskildsen-Larsen, S., Rebouillat, D., Paludan, S. R., Sen, G., Williams, B. R., and Hartmann, R. (2008) The p59 oligoadenylate synthetase-like protein possesses antiviral activity that requires the C-terminal ubiquitin-like domain. *The Journal of general virology* 89, 2767-2772
45. Dong, B., Zhou, Q., Zhao, J., Zhou, A., Harty, R. N., Bose, S., Banerjee, A., Slee, R., Guenther, J., Williams, B. R., Wiedmer, T., Sims, P. J., and Silverman, R. H. (2004) Phospholipid scramblase 1 potentiates the antiviral activity of interferon. *Journal of virology* 78, 8983-8993
46. Unterholzner, L., Keating, S. E., Baran, M., Horan, K. A., Jensen, S. B., Sharma, S., Sirois, C. M., Jin, T., Latz, E., Xiao, T. S., Fitzgerald, K. A., Paludan, S. R., and Bowie, A. G. (2010) IFI16 is an innate immune sensor for intracellular DNA. *Nature immunology* 11, 997-1004
47. Nakatsu, F., and Ohno, H. (2003) Adaptor protein complexes as the key regulators of protein sorting in the post-Golgi network. *Cell Struct Funct* 28, 419-429
48. Lau, A. W., and Chou, M. M. (2008) The adaptor complex AP-2 regulates post-endocytic trafficking through the non-clathrin Arf6-dependent endocytic pathway. *Journal of cell science* 121, 4008-4017
49. McCormick, P. J., Martina, J. A., and Bonifacino, J. S. (2005) Involvement of clathrin and AP-2 in the trafficking of MHC class II molecules to antigen-processing compartments. *Proceedings of the National Academy of Sciences of the United States of America* 102, 7910-7915
50. Rufer, E., Leonhardt, R. M., and Knittler, M. R. (2007) Molecular architecture of the TAP-associated MHC class I peptide-loading complex. *Journal of immunology* 179, 5717-5727
51. Kondos, S. C., Hatfaludi, T., Voskoboinik, I., Trapani, J. A., Law, R. H. P., Whisstock, J. C., and Dunstone, M. A. (2010) The structure and function of mammalian membrane-attack complex/perforin-like proteins. *Tissue Antigens* 76, 341-351
52. Triantafilou, K., Hughes, T. R., Triantafilou, M., and Morgan, B. P. (2013) The complement membrane attack complex triggers intracellular Ca2+ fluxes leading to NLRP3 inflammasome activation. *Journal of cell science* 126, 2903-2913
53. Ishigaki, Y., Li, X., Serin, G., and Maquat, L. E. (2001) Evidence for a pioneer round of mRNA translation: mRNAs subject to nonsense-mediated decay in mammalian cells are bound by CBP80 and CBP20. *Cell* 106, 607-617
54. Woeller, C. F., Gaspari, M., Isken, O., and Maquat, L. E. (2008) NMD resulting from encephalomyocarditis virus IRES-directed translation initiation seems to be restricted to CBP80/20-bound mRNA. *EMBO reports* 9, 446-451

55. Jenkins, K., Khoo, J. J., Sadler, A., Piganis, R., Wang, D., Borg, N. A., Hjerrild, K., Gould, J., Thomas, B. J., Nagley, P., Hertzog, P. J., and Mansell, A. (2013) Mitochondrially localised MUL1 is a novel modulator of antiviral signaling. *Immunol Cell Biol* 91, 321-330
56. Cheng, H., Cenciarelli, C., Nelkin, G., Tsan, R., Fan, D., Cheng-Mayer, C., and Fidler, I. J. (2005) Molecular mechanism of hTid-1, the human homolog of Drosophila tumor suppressor l(2)Tid, in the regulation of NF-kappaB activity and suppression of tumor growth. *Molecular and cellular biology* 25, 44-59
57. Guillot, L., Le Goffic, R., Bloch, S., Escriou, N., Akira, S., Chignard, M., and Si-Tahar, M. (2005) Involvement of toll-like receptor 3 in the immune response of lung epithelial cells to double-stranded RNA and influenza A virus. *The Journal of biological chemistry* 280, 5571-5580
58. Takeuchi, O., and Akira, S. (2010) Pattern recognition receptors and inflammation. *Cell* 140, 805-820
59. Miyamoto, M., Fujita, T., Kimura, Y., Maruyama, M., Harada, H., Sudo, Y., Miyata, T., and Taniguchi, T. (1988) Regulated expression of a gene encoding a nuclear factor, IRF-1, that specifically binds to IFN-beta gene regulatory elements. *Cell* 54, 903-913
60. Ohgaki, R., Matsushita, M., Kanazawa, H., Ogihara, S., Hoekstra, D., and van Ijzendoorn, S. C. (2010) The Na+/H+ exchanger NHE6 in the endosomal recycling system is involved in the development of apical bile canalicular surface domains in HepG2 cells. *Molecular biology of the cell* 21, 1293-1304
61. Saint-Pol, A., Bauvy, C., Codogno, P., and Moore, S. E. (1997) Transfer of free polymannose-type oligosaccharides from the cytosol to lysosomes in cultured human hepatocellular carcinoma HepG2 cells. *The Journal of cell biology* 136, 45-59
62. Hsu, M. H., Savas, U., Griffin, K. J., and Johnson, E. F. (2001) Identification of peroxisome proliferator-responsive human genes by elevated expression of the peroxisome proliferator-activated receptor alpha in HepG2 cells. *The Journal of biological chemistry* 276, 27950-27958
63. De Duve, C., Pressman, B. C., Gianetto, R., Wattiaux, R., and Appelmans, F. (1955) Tissue fractionation studies. 6. Intracellular distribution patterns of enzymes in rat-liver tissue. *Biochem J* 60, 604-617
64. Bonifacino, J., Dasso, M., Harford, J., Lippincott-Schwartz, J., and Yamada, K. (2004) Short protocols in cell biology. *QH585* 2, S46
65. Wanders, R. J., and Waterham, H. R. (2006) Biochemistry of mammalian peroxisomes revisited. *Annual review of biochemistry* 75, 295-332
66. Emmett, S. R., Dove, B., Mahoney, L., Wurm, T., and Hiscox, J. A. (2005) The cell cycle and virus infection. *Methods in molecular biology* 296, 197-218
67. Whyte, P., Williamson, N. M., and Harlow, E. (1989) Cellular targets for transformation by the adenovirus E1A proteins. *Cell* 56, 67-75
68. Dyson, N., Howley, P. M., Munger, K., and Harlow, E. (1989) The human papilloma virus-16 E7 oncoprotein is able to bind to the retinoblastoma gene product. *Science* 243, 934-937
69. Lin, G. Y., and Lamb, R. A. (2000) The paramyxovirus simian virus 5 V protein slows progression of the cell cycle. *Journal of virology* 74, 9152-9166
70. Ehmann, G. L., McLean, T. I., and Bachenheimer, S. L. (2000) Herpes simplex virus type 1 infection imposes a G(1)/S block in asynchronously growing cells and prevents G(1) entry in quiescent cells. *Virology* 267, 335-349
71. Dittmer, D., and Mocarski, E. S. (1997) Human cytomegalovirus infection inhibits G1/S transition. *Journal of virology* 71, 1629-1634
72. Re, F., Braaten, D., Franke, E. K., and Luban, J. (1995) Human immunodeficiency virus type 1 Vpr arrests the cell cycle in G2 by inhibiting the activation of p34cdc2-cyclin B. *Journal of virology* 69, 6859-6864

73. Kannan, R. P., Hensley, L. L., Evers, L. E., Lemon, S. M., and McGivern, D. R. (2011) Hepatitis C virus infection causes cell cycle arrest at the level of initiation of mitosis. *Journal of virology* 85, 7989-8001
74. Naniche, D., Reed, S. I., and Oldstone, M. B. (1999) Cell cycle arrest during measles virus infection: a G0-like block leads to suppression of retinoblastoma protein expression. *Journal of virology* 73, 1894-1901
75. Dohner, K., and Sodeik, B. (2005) The role of the cytoskeleton during viral infection. *Current topics in microbiology and immunology* 285, 67-108
76. Honer, B., and Jockusch, B. M. (1988) Stress fiber dynamics as probed by antibodies against myosin. *European journal of cell biology* 47, 14-21
77. Sasaki, H., Nakamura, M., Ohno, T., Matsuda, Y., Yuda, Y., and Nonomura, Y. (1995) Myosin-actin interaction plays an important role in human immunodeficiency virus type 1 release from host cells. *Proceedings of the National Academy of Sciences of the United States of America* 92, 2026-2030
78. Bukrinskaya, A., Brichacek, B., Mann, A., and Stevenson, M. (1998) Establishment of a functional human immunodeficiency virus type 1 (HIV-1) reverse transcription complex involves the cytoskeleton. *The Journal of experimental medicine* 188, 2113-2125
79. Ada-Nguema, A. S., Xenias, H., Hofman, J. M., Wiggins, C. H., Sheetz, M. P., and Keely, P. J. (2006) The small GTPase R-Ras regulates organization of actin and drives membrane protrusions through the activity of PLCepsilon. *Journal of cell science* 119, 1307-1319
80. Aresta, S., de Tand-Heim, M. F., Beranger, F., and de Gunzburg, J. (2002) A novel Rho GTPase-activating-protein interacts with Gem, a member of the Ras superfamily of GTPases. *Biochem J* 367, 57-65
81. Wilkinson, S., Paterson, H. F., and Marshall, C. J. (2005) Cdc42-MRCK and Rho-ROCK signalling cooperate in myosin phosphorylation and cell invasion. *Nature cell biology* 7, 255-261
82. Ohman, T., Rintahaka, J., Kalkkinen, N., Matikainen, S., and Nyman, T. A. (2009) Actin and RIG-I/MAVS signaling components translocate to mitochondria upon influenza A virus infection of human primary macrophages. *Journal of immunology* 182, 5682-5692
83. An, K., Fang, L., Luo, R., Wang, D., Xie, L., Yang, J., Chen, H., and Xiao, S. (2014) Quantitative Proteomic Analysis Reveals That Transmissible Gastroenteritis Virus Activates the JAK-STAT1 Signaling Pathway. *Journal of proteome research* 13, 5376-5390
84. Fan, H., Ye, Y., Luo, Y., Tong, T., Yan, G., and Liao, M. (2012) Quantitative proteomics using stable isotope labeling with amino acids in cell culture reveals protein and pathway regulation in porcine circovirus type 2 infected PK-15 cells. *Journal of proteome research* 11, 995-1008
85. Zheng, X., Hong, L., Shi, L., Guo, J., Sun, Z., and Zhou, J. (2008) Proteomics analysis of host cells infected with infectious bursal disease virus. *Molecular & cellular proteomics : MCP* 7, 612-625
86. Basrur, V., Yang, F., Kushimoto, T., Higashimoto, Y., Yasumoto, K., Valencia, J., Muller, J., Vieira, W. D., Watabe, H., Shabanowitz, J., Hearing, V. J., Hunt, D. F., and Appella, E. (2003) Proteomic analysis of early melanosomes: identification of novel melanosomal proteins. *Journal of proteome research* 2, 69-79
87. Yabe, D., Nakamura, T., Kanazawa, N., Tashiro, K., and Honjo, T. (1997) Calumenin, a Ca2+-binding protein retained in the endoplasmic reticulum with a novel carboxyl-terminal sequence, HDEF. *The Journal of biological chemistry* 272, 18232-18239
88. Wang, Q., Feng, H., Zheng, P., Shen, B., Chen, L., Liu, L., Liu, X., Hao, Q., Wang, S., Chen, J., and Teng, J. (2012) The intracellular transport and secretion of calumenin-1/2 in living cells. *PloS one* 7, e35344
89. Fornarini, B., D'Ambrosio, C., Natoli, C., Tinari, N., Silingardi, V., and Iacobelli, S. (2000) Adhesion to 90K (Mac-2 BP) as a mechanism for lymphoma drug resistance in vivo. *Blood* 96, 3282-3285

90. Iacobelli, S., Sismondi, P., Giai, M., D'Egidio, M., Tinari, N., Amatetti, C., Di Stefano, P., and Natoli, C. (1994) Prognostic value of a novel circulating serum 90K antigen in breast cancer. *British journal of cancer* 69, 172-176
91. Marchetti, A., Tinari, N., Buttitta, F., Chella, A., Angeletti, C. A., Sacco, R., Mucilli, F., Ullrich, A., and Iacobelli, S. (2002) Expression of 90K (Mac-2 BP) correlates with distant metastasis and predicts survival in stage I non-small cell lung cancer patients. *Cancer research* 62, 2535-2539
92. Strizzi, L., Muraro, R., Vianale, G., Natoli, C., Talone, L., Catalano, A., Mutti, L., Tassi, G., and Procopio, A. (2002) Expression of glycoprotein 90K in human malignant pleural mesothelioma: correlation with patient survival. *The Journal of pathology* 197, 218-223
93. Ullrich, A., Sures, I., D'Egidio, M., Jallal, B., Powell, T. J., Herbst, R., Dreps, A., Azam, M., Rubinstein, M., Natoli, C., and et al. (1994) The secreted tumor-associated antigen 90K is a potent immune stimulator. *The Journal of biological chemistry* 269, 18401-18407
94. Warke, R. V., Becerra, A., Zawadzka, A., Schmidt, D. J., Martin, K. J., Giaya, K., Dinsmore, J. H., Woda, M., Hendricks, G., Levine, T., Rothman, A. L., and Bosch, I. (2008) Efficient dengue virus (DENV) infection of human muscle satellite cells upregulates type I interferon response genes and differentially modulates MHC I expression on bystander and DENV-infected cells. *The Journal of general virology* 89, 1605-1615
95. Li, J., Shen, H., Himmel, K. L., Dupuy, A. J., Largaespada, D. A., Nakamura, T., Shaughnessy, J. D., Jr., Jenkins, N. A., and Copeland, N. G. (1999) Leukaemia disease genes: large-scale cloning and pathway predictions. *Nature genetics* 23, 348-353
96. Leegwater, P. A., Konst, A. A., Kuyt, B., Sandkuijl, L. A., Naidu, S., Oudejans, C. B., Schutgens, R. B., Pronk, J. C., and van der Knaap, M. S. (1999) The gene for leukoencephalopathy with vanishing white matter is located on chromosome 3q27. *American journal of human genetics* 65, 728-734
97. Vitols, S., Gahrton, G., Bjorkholm, M., and Peterson, C. (1985) Hypocholesterolaemia in malignancy due to elevated low-density-lipoprotein-receptor activity in tumour cells: evidence from studies in patients with leukaemia. *Lancet* 2, 1150-1154
98. Cable, S., Keller, J. M., Colin, S., Haffen, K., Kedinger, M., Parache, R. M., and Dauca, M. (1992) Peroxisomes in human colon carcinomas. A cytochemical and biochemical study. *Virchows Archiv. B, Cell pathology including molecular pathology* 62, 221-226
99. Zhao, S., Xu, W., Jiang, W., Yu, W., Lin, Y., Zhang, T., Yao, J., Zhou, L., Zeng, Y., Li, H., Li, Y., Shi, J., An, W., Hancock, S. M., He, F., Qin, L., Chin, J., Yang, P., Chen, X., Lei, Q., Xiong, Y., and Guan, K. L. (2010) Regulation of cellular metabolism by protein lysine acetylation. *Science* 327, 1000-1004
100. Sacksteder, K. A., Jones, J. M., South, S. T., Li, X., Liu, Y., and Gould, S. J. (2000) PEX19 binds multiple peroxisomal membrane proteins, is predominantly cytoplasmic, and is required for peroxisome membrane synthesis. *The Journal of cell biology* 148, 931-944
101. Kim, P. K., Mullen, R. T., Schumann, U., and Lippincott-Schwartz, J. (2006) The origin and maintenance of mammalian peroxisomes involves a de novo PEX16-dependent pathway from the ER. *The Journal of cell biology* 173, 521-532
102. Honsho, M., Hiroshige, T., and Fujiki, Y. (2002) The membrane biogenesis peroxin Pex16p. Topogenesis and functional roles in peroxisomal membrane assembly. *The Journal of biological chemistry* 277, 44513-44524

Figure legends

Figure 1. The quantitative proteomic analysis of the peroxisome-density-like fraction in the SeV-infected HepG2 cells.

(A) The proteomic work flow. (B) The correlation of these three biological repeats, the Pearson correlation factors are 0.7866, 0.5865 and 0.6316 respectively. (C) Gaussian distribution of the quantitative date, the mean value was 0.0062 and SD value was 0.315. The mean ± 1.96 SD cutoffs are marked with a dashed line. The up-regulated cutoff was 1.542 and the down-regulated cutoff was 0.654. (D) The subcellular annotation of the PEFs proteins of the HepG2 cells upon SeV infection. The subcellular localization of the total quantitated proteins (n=2946), the up-regulated proteins (n=99) and the down-regulated proteins (n=212). The localization information was obtained from Gene Ontology. The detailed information can be seen in Table S4.

Figure 2. The Statistical enrichment test results based on the biological process annotations.

Protein ratio list were uploaded to PANTHER website for statistical enrichment test. Only the significantly changed categories ($p < 0.05$) were shown. The p value of each category was indicated by red words. Based on the biological process annotations, these following categories were shown in the figure, (A) Protein localization to ER, (B) Viral life cycle, (C) Extracellular structure, (D) Viral transcription, (E) Cell cycle process, (F) Microtubule-based process, (G) mRNA processing, (H) Peroxisome organization. The detailed information can be seen in Table S5. The X axis is protein ratio (log_2 value), Y axis is the certain protein' ratio higher than how many percent (percent/100) of proteins in the indicated protein group.

Figure 3. The Statistical enrichment test results based on the molecular function annotations.

Protein ratio list were uploaded to PANTHER website for statistical enrichment test. Only the significantly changed categories ($p < 0.05$) were shown. The p value of each category was indicated by red words. Based on the molecular function annotations, these following categories were shown in the figure, (A) Oxidoreductase activity, (B) Clathrin binding, (C) Motor activity, (D) Nucleotide binding, (E) Small molecule binding. The detailed information can be seen in Table S5. The axis annotations refer to Fig. 2.

Figure 4. An overview of the specific functional networks.

A global view of the significantly regulated proteins following SeV infection. The SeV infection-regulated proteins were grouped into different categories based on their functions or cellular components, as annotated by PANTHER, KEGG and UniProt databases. The red and blue fractions belong to the up- and down-regulated groups, respectively. The detailed information can be seen in Table S6.

Figure 5. A screen for potential antiviral innate immune-related proteins.

(A) The effects of the overexpressed candidate proteins on SeV-triggered activation of the IFN-β promoter. 293 cells (2×10^5) were transfected with the IFN-β promoter reporter (0.1 μg) and the indicated expression plasmid (0.5-μg each). Twenty-four hours after the transfection, the cells were infected with SeV for 12 hours or left uninfected before the reporter assays were performed. (B) The effects of the overexpressed candidate proteins on SeV-triggered activation of the ISRE promoter. Luciferase reporter assays were performed as described in (A). (C) The effects of the overexpressed candidate proteins on SeV-triggered activation of the NF-κB promoter. Luciferase reporter assays were performed as described in (A). (D) The effects of the overexpressed candidate proteins on the IFN-γ-triggered activation of the IRF-1 promoter. Luciferase reporter assays were performed as described in (A). The data shown are

averages and standard deviations of one representative experiment performed independently in triplicates. The results are shown as the mean ± S.D.

Figure 6. The luciferase reporter assays of the dose-dependent overexpression of the candidate proteins.

(A, B, E and F) The effects of the overexpression of CALU, LGALS3BP, EHHADH and PEX16 on SeV-triggered activation of the IFN-β, ISRE and NF-κB reporter. 293 cells (2×10^5) were transfected with the IFN-β promoter reporter (0.1 μg), NF-κB reporter (0.1 μg) or ISRE promoter reporter (0.1 μg) together with a control or the indicated expression plasmid (0.1, 0.2 or 0.5 μg), respectively. Twenty-four hours after the transfection, the cells were infected with SeV for 12 hours at an MOI of 100 or left uninfected before the reporter assays were performed. (C, D, G and H) The effects of the overexpression of CALU, LGALS3BP, EHHADH and PEX16 on the IFN-γ-triggered activation of the IRF-1 promoter. 293 cells (2×10^5) were transfected with the IRF-1 promoter reporter (0.1 μg) together with a control or the indicated expression plasmid (0.1, 0.2 or 0.5 μg), respectively. Twenty-four hours after the transfection, the cells were treated with IFN-γ (final concentration 100 ng/ml) for 12 hours or left untreated before the reporter assays were performed. The data shown are averages and standard deviations of one representative experiment performed independently in triplicates. The results are shown as the mean ± S.D. *, $p < 0.01$ relative to the control.

Figure 7. Knockdown of CALU and LGALS3BP positively regulate SeV-induced activation of IFN-β in a dose-dependent manner.

(A, and B) The effects of CALU and LGALS3BP knockdown on SeV-triggered induction of the *IFNB1* gene and the knockdown efficiency of each gene. The effects of CALU and LGALS3BP knockdown on SeV-induced production of IFN-β protein. 293 cells (2×10^5) were transfected with a control or the

indicated siRNA (1 μg). Twenty-four hours after the transfection, the cells were infected with SeV for 12 hours at an MOI of 100 or left uninfected, followed by quantitative real-time PCR. For ELISA analysis, the cells were infected with SeV for 16 hours at an MOI of 100 or left uninfected. (C, and D) The western blot analysis of knockdown efficiency of CALU and LGALS3BP, 293 cells (2×10^5) were transfected with indicated expression plasmid (0.5 μg) together with a control or the indicated siRNA (1 μg). HA-actin plasmid (0.5 μg) was transfected as internal control. Bands quantified by Quantity One software. (E, and F) The effects of CALU and LGALS3BP knockdown on SeV-triggered activation of the IFN-β, ISRE and NF-κB reporter. 293 cells (2×10^5) were transfected with the IFN-β promoter or ISRE reporter (0.1 μg) together with a control or siRNA (1 μg). Luciferase reporter assays were performed as described in Fig. 6. (G, and H) The effects of CALU and LGALS3BP knockdown on the IFN-γ-triggered activation of the IRF-1 promoter. 293 cells (2×10^5) were transfected with the IRF-1 promoter reporter (0.1 μg) together with a control or siRNA (1 μg). Luciferase reporter assays were performed as described in Fig. 6. Western blot analysis was repeated for at least three times with similar results. The data shown are averages and standard deviations of one representative experiment performed independently in triplicates. The results are shown as the mean ± S.D. *, $p < 0.01$ relative to the control.

g. 1

A

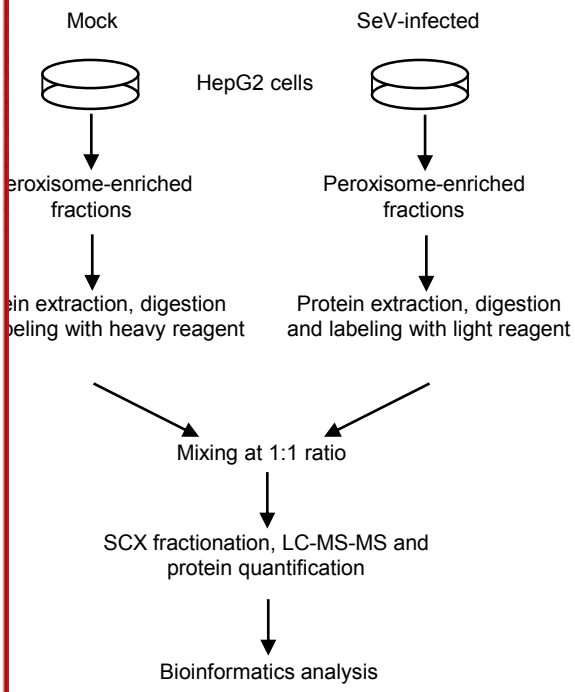

B

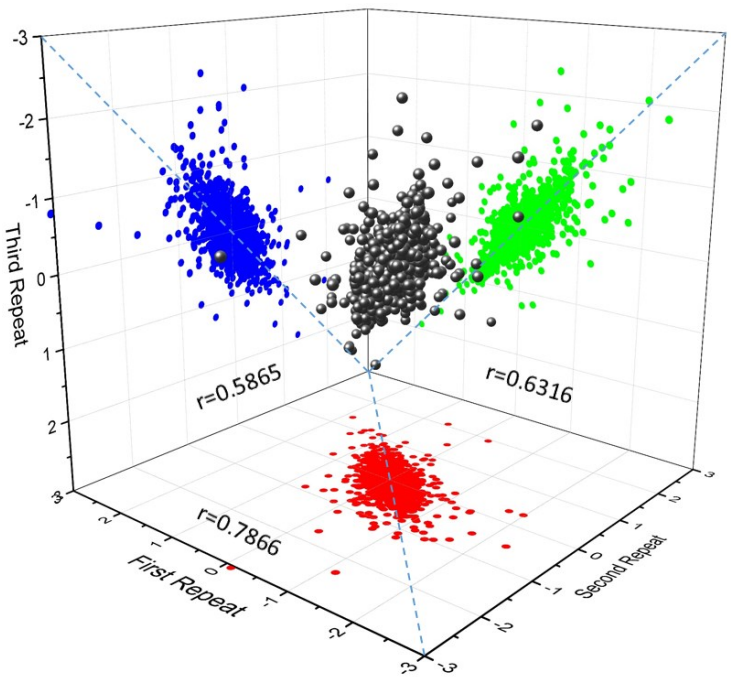

C

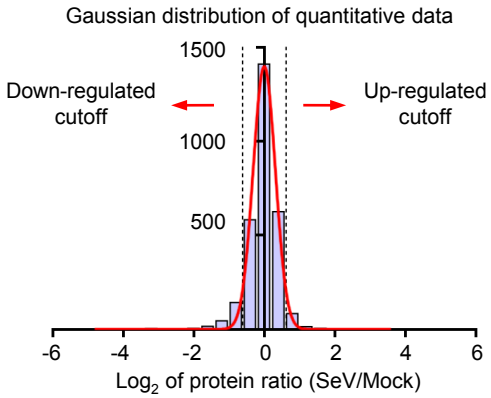

D

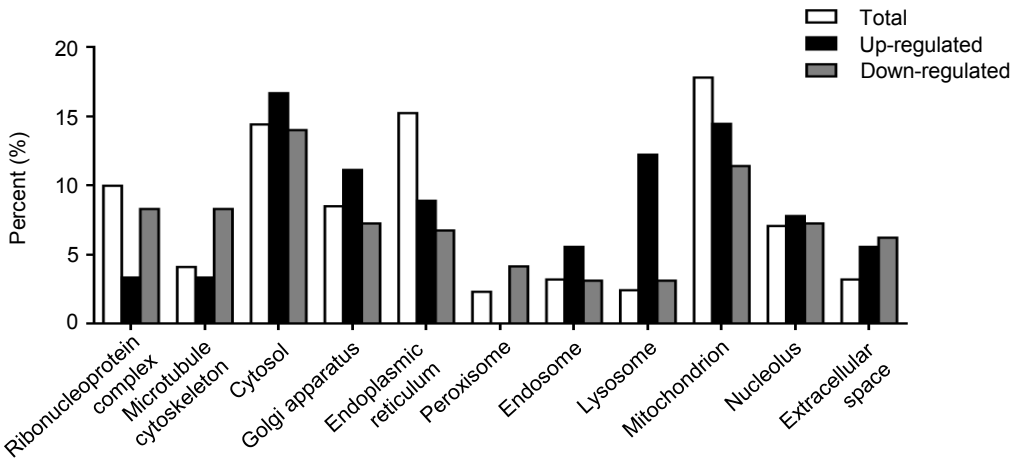

g. 2

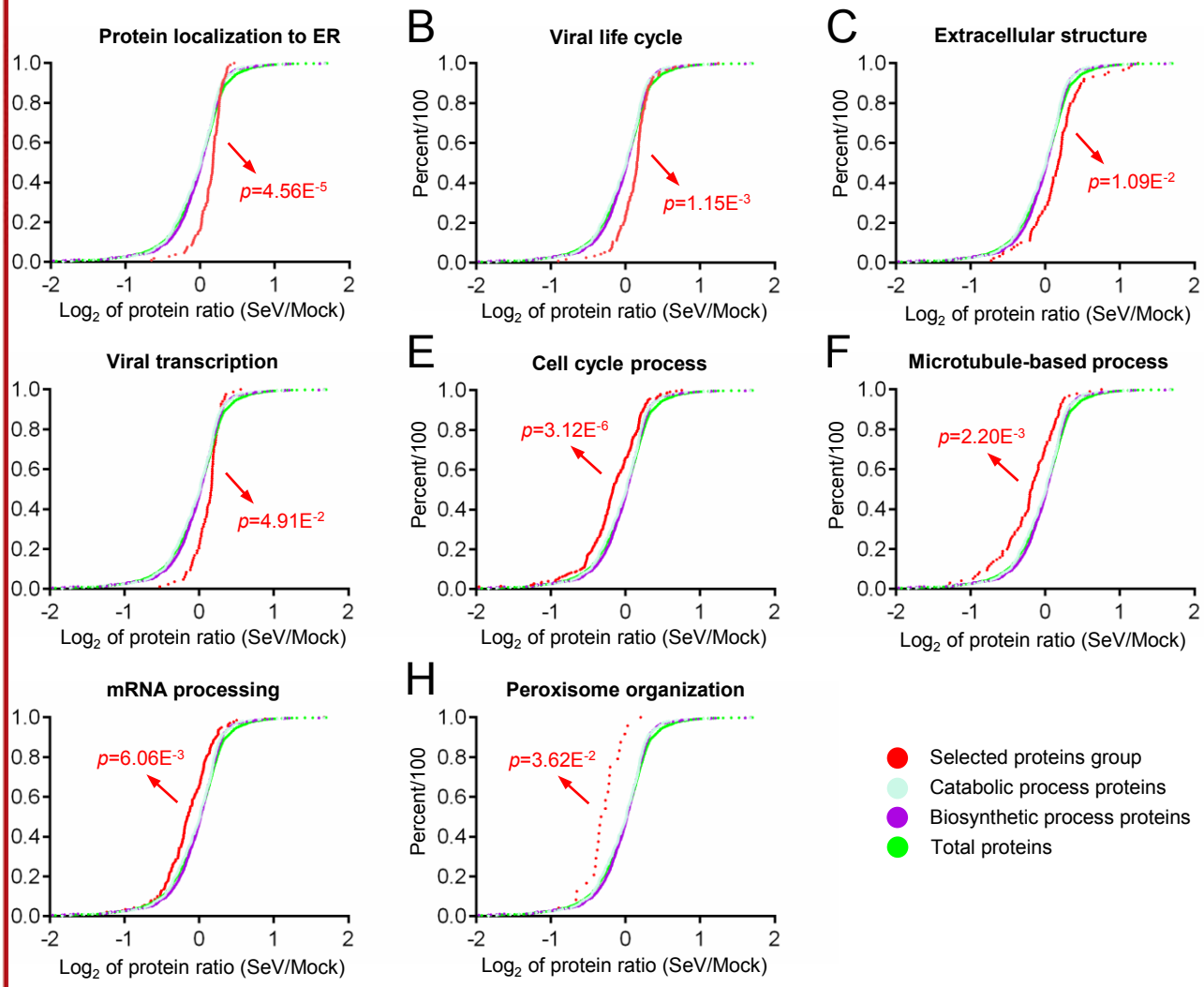

ASBMB MOLECULAR & CELLULAR PROTEOMICS MCP

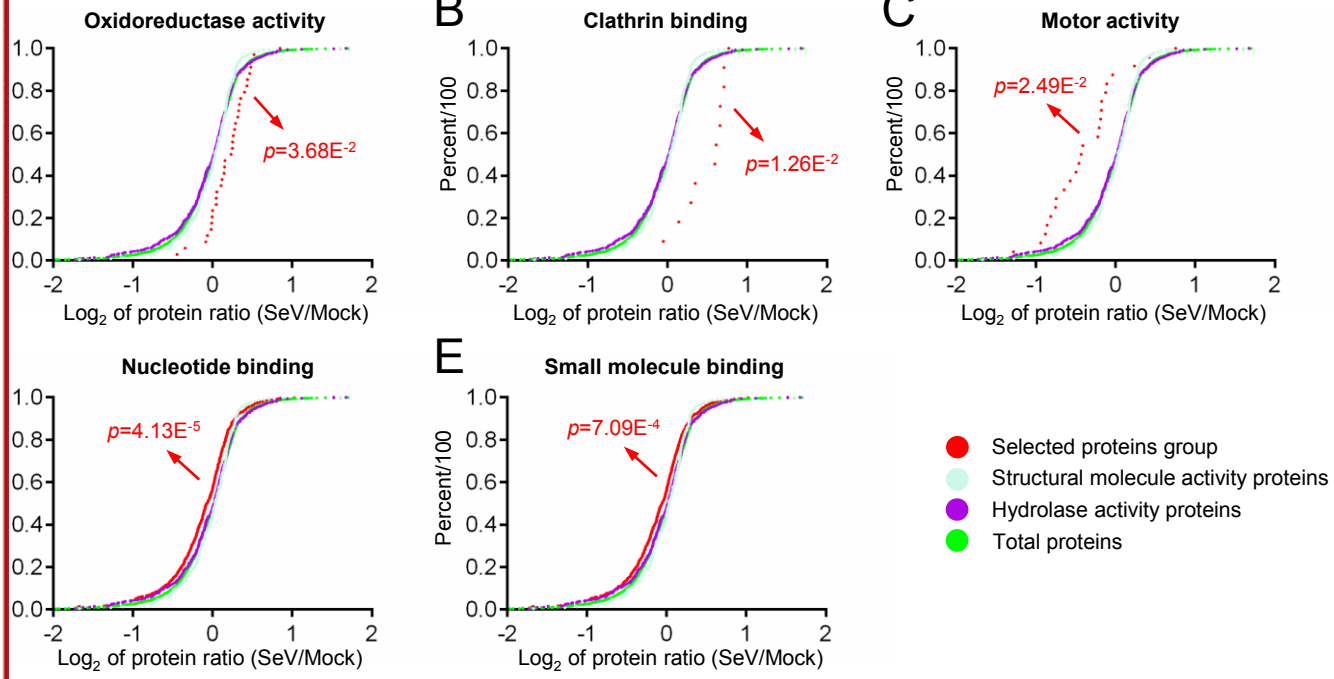

g. 4

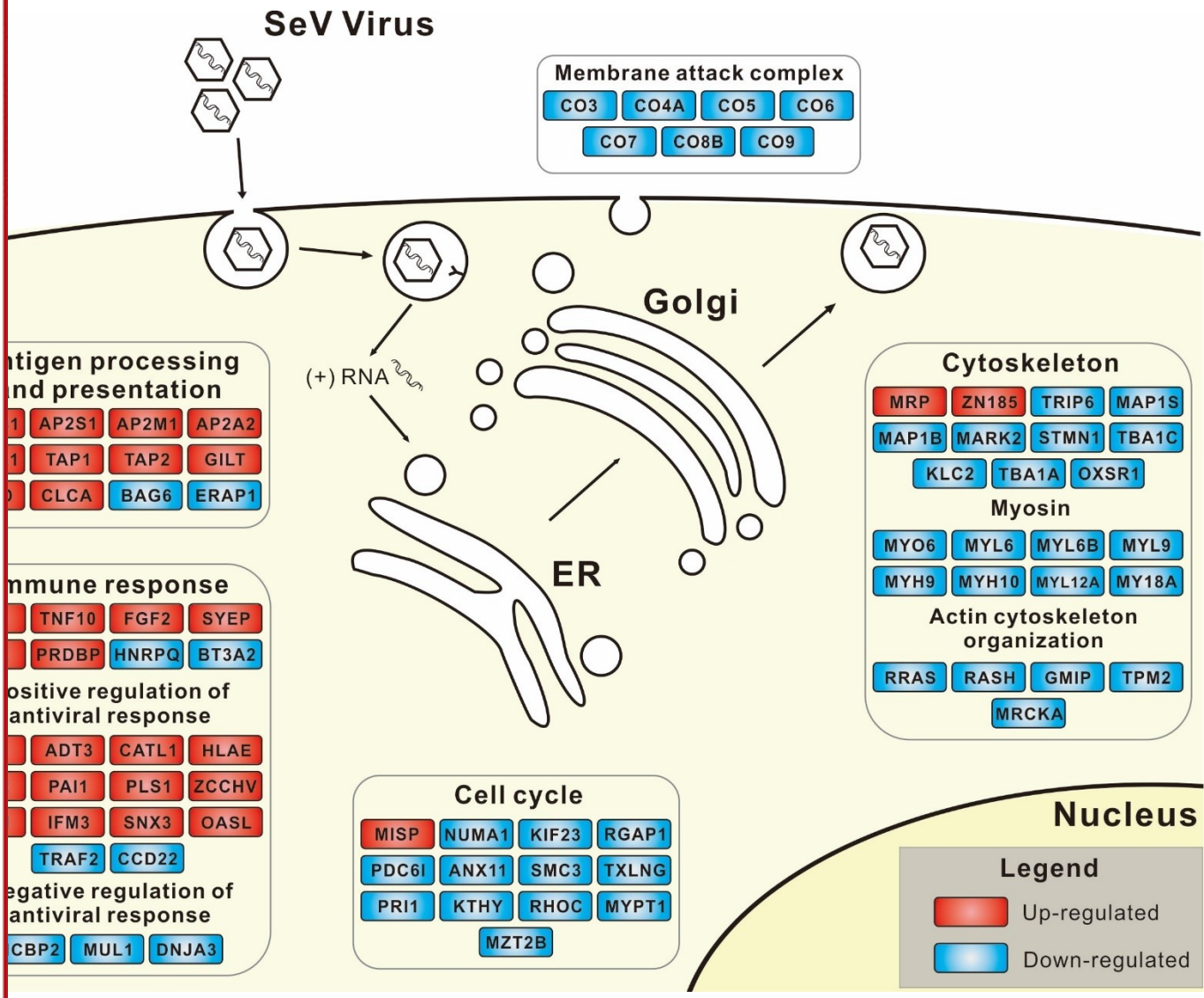

g. 5

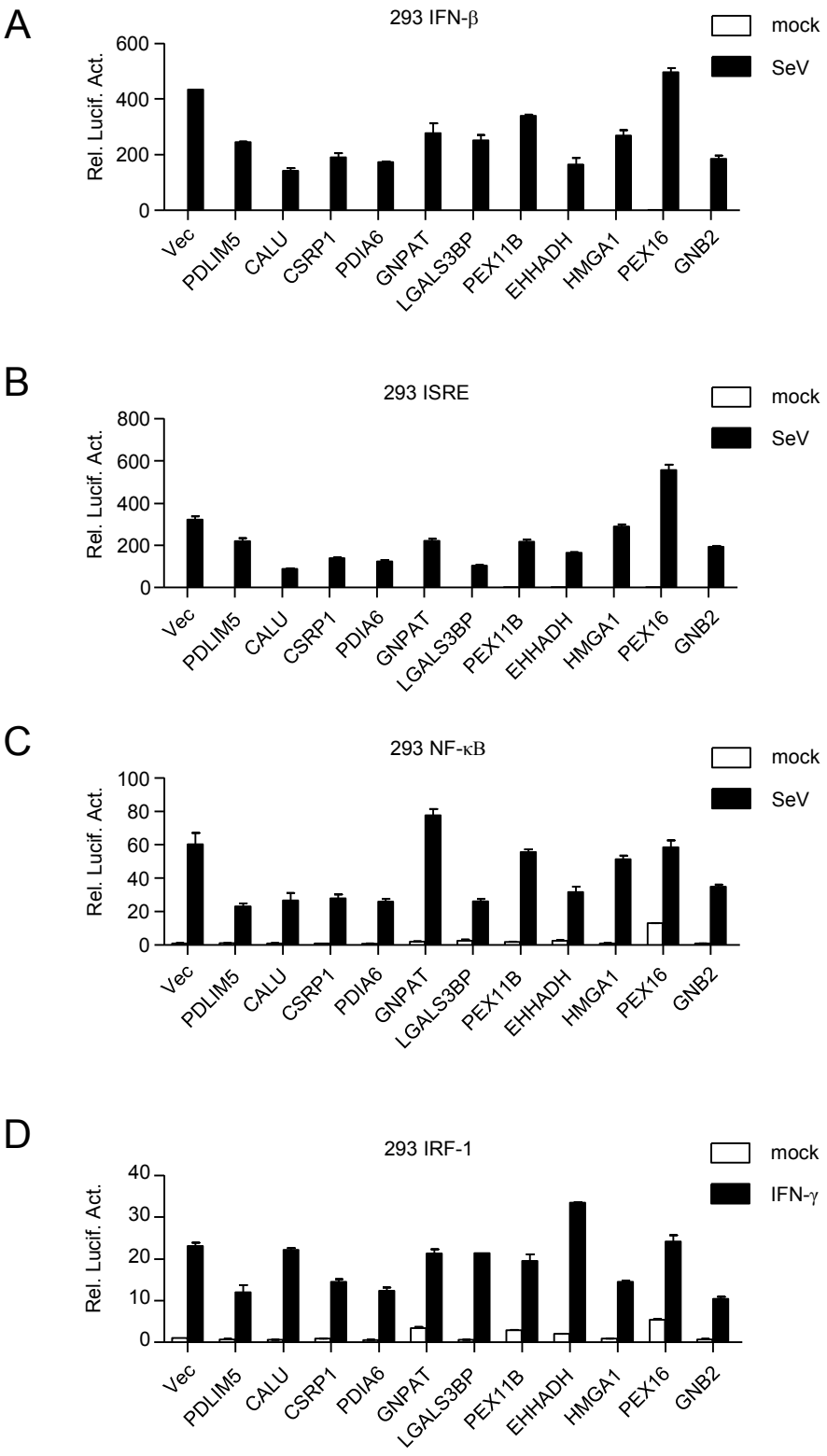

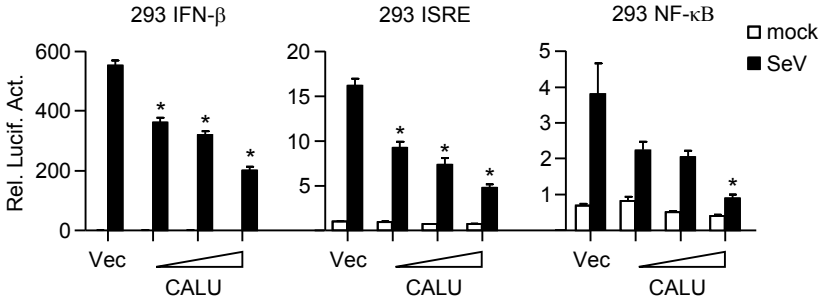

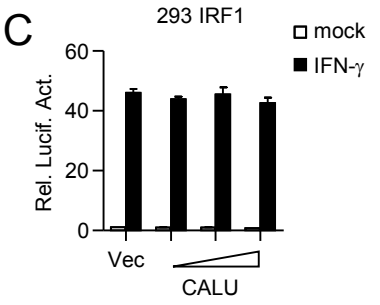

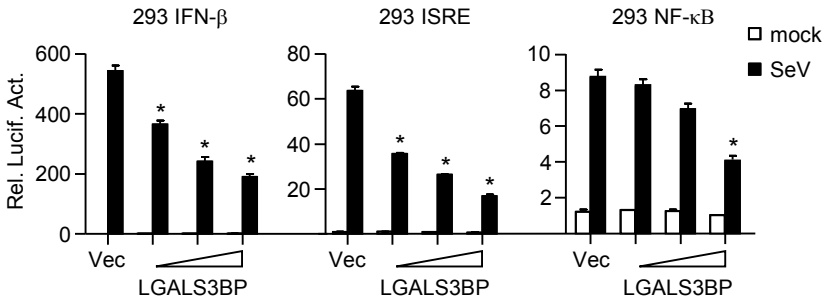

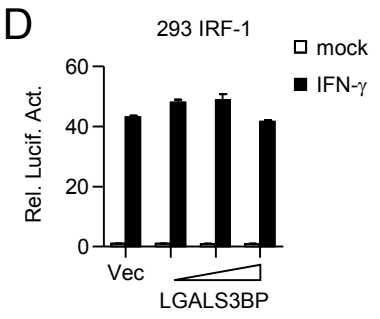

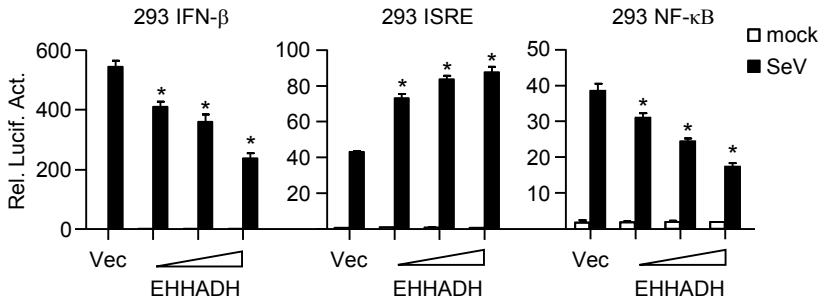

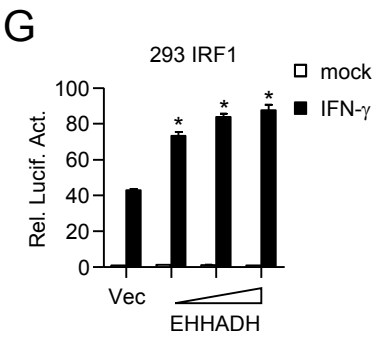

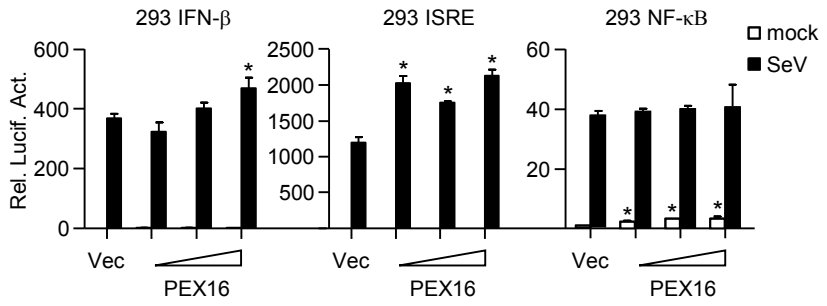

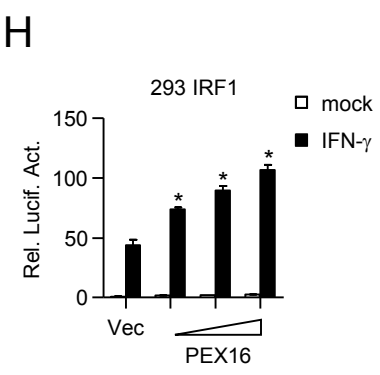

g. 7